Original Article

Bulletin of Pure and Applied Sciences.
Vol.38 C (Chemistry), No.1, 2019: P.40-59
Print version ISSN 0970 4620
Online version ISSN 2320 320X
DOI 10.5958/2320-320X.2019.00005.0
http://www.bpasjournals.com/chemistry/

Spectroscopic (IR, UV, NMR) characterization of 4, 8 -di methyl 2, 6 -di phenyl 1, 5 -di hydro S-Indacene and study of effect of substituents in its electronic properties

I. Pushpavathi[1],
K.M. Mussavir Pasha[2],
S. Muthu[3],
M.K. Amshumali[4]*

Author Affiliations
[1,2,4]Department of Chemistry/Industrial Chemistry, Vijayanagara Sri Krishnadevaraya University, Jnanasagara Campus, Cantonment, Ballari, Karnataka 583104, India
[3]Department of Physics, Arignar Anna Govt.Arts College, Cheyyar,, Tamil Nadu 604407, India

***Corresponding Author**
M.K. Amshumali, Department of Chemistry/Industrial Chemistry, Vijayanagara Sri Krishnadevaraya University, Jnanasagara Campus, Cantonment, Ballari, Karnataka 583104, India

E-mail:
amshumali@vskub.ac.in,
amshumali.m@gmail.com

Received on 19.10.2018
Accepted on 12.12.2018

Abstract

In the present study, quantum computational methods such as semi empirical, Hartree fock and density functional theory (DFT) are used for the analysis of molecular structure of 4, 8-di methyl, 2, 6 - di phenyl, 1, 5 - di hydro S-Indacene. Vibrational analysis was carried out using DFT method with the basis set B3LYP/6–31G (d, p) and the infrared and Raman spectra of title compound were reported. Frequency assignments of the vibration spectra were carried out with potential energy distribution (PED). Optimization of the title compound were calculated by the methods AM1, PM6, HF/6-31G and B3LYP/6-31G (d, p) basis set in gas phase. Furthermore, effect of substituents of the title molecule on its electronic properties such as HOMO-LUMO energy gap, absorption maxima and oscillator strengths in UV-Vis spectrum, NBO analysis, TDOS, Fukui function and the local softness and eletrophilicity indices were calculated. The thermodynamic properties have also been calculated and predicted the relationship of these properties with temperature.

Keywords: Semi empirical methods, S-indacene, Fukui function, Electrophilicity indices, B3YLP.

1. Introduction

In chemistry of anti-aromatic molecules that contains 12 pi electron, S-indacene is attracted a considerable interest as a ligand. Because of its ability for the formation of bridged ligand metallic complexes. Nonetheless it has structural features that have long puzzled experimentalists and theoreticians. The parent molecule is highly reactive and has not been characterized experimentally due to its instability[1]. S-indacene should be stabilized by donor groups in the 4, 8 position and acceptor groups in the 2, and 6 positions. Such type of compounds with substitution are 4, 8-bis (dimethylamino)-s-indacene, which has a delocalized pi-electron system and accordingly should be described as an anti- aromatic (4n) ɪɪ-system. S-indacene substituted derivatives are represented in the figure 1.

A literature survey reveals that, Except few papers by S. Muthu *et al* [2-4] are reported the theoretical calculations such as geometry optimization and spectroscopic characterization and properties for some known compounds, none is reported for 4, 8- di methyl 2, 6- di phenyl 1, 5 - di hydro S-

Indacene so far. Therefore, in the present study we aimed to give information of optimized geometry, molecular vibrations and electronic features of the title molecule. Furthermore, we also investigated the effect of substituent on the electronic properties of s- Indacene. We also report the theoretical vibrational assignment for the fundamental bands in Infra Red spectrum, Fukui function calculation, NBO analysis, linear polarizability (α) and the first order hyperpolarizability (β) values of the title molecule.

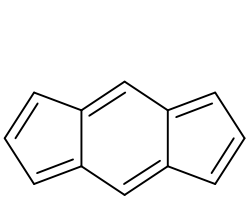

s-indacene

1(A)

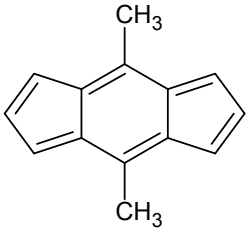

4,8-dimethyl-*s*-indacene

1(B)

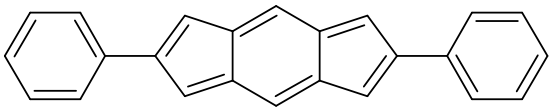

2,6-diphenyl-*s*-indacene

1(C)

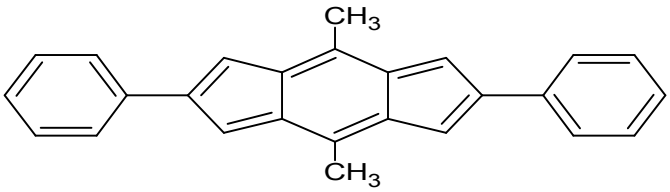

4,8-dimethyl-2,6-diphenyl-*s*-indacene

1(D)

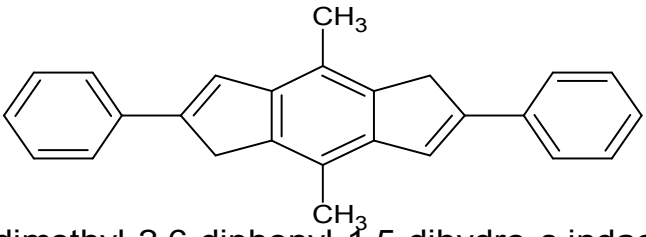

4,8-dimethyl-2,6-diphenyl-1,5-dihydro-*s*-indacene

1(E)

Figure 1: (A) S-Indacene **1(B)** 4,8 di methyl indacene **1 (C)** 2,6 di phenyl Indacene
1(D) 4,8 di methyl 2,6 di phenyl Indacene **1(E)** 4,8 di methyl 2,6 di phenyl 1,5 di hydro Indacene

2. Computational details

All computational calculations were carried using Hybrid methods B3YLP with 6-31G (d, p) basis set of the DFT using gradient geometry optimization [5-7]. All the computations were performed using Gaussian 09 program and Gauss-view and Chemcraft as molecular visualization program[6]. Vibrational frequency assignments are made with a high degree of confidence with PED using VEDA program and defined coordinates match quite well with the vibrational motions in the GAUSSVIEW

program. The study of molecular group contributions to orbitals, the total density of states (TDOS) and sum of alpha and beta density of states (αβDOS) spectra were prepared by using the program Gaussum 2.2.5. The TDOS and αβDOS spectra were created by convoluting the molecular orbital information with Gaussian curves of unit height and a FWHM (Full Width at Half Maximum) of 0.3ev. NBO analysis was carried out to study the Donor-Acceptor interactions in title molecule. Fukui function calculations were used for finding the local parameters like local softness and electrophilicity indices using UCA –FUKUI software.

3. Results and discussion

3.1. Geometrical structure

The geometry optimization of 4, 8- di methyl,2, 6 - di phenyl 1, 5- di hydro S-Indacene is carried out using PM3, AM1,HF and DFT methods using Gaussian 09 software in gas phase. The labeling of atoms in title molecule ($C_{26}H_{22}$) given in Fig. 2. Geometrical parameters such as bond lengths and bond angles of title compound were calculated. All geometry parameters of optimized structure determined by four methods (AM1, PM6, HF and DFT) and summarized bond lengths were listed in Table 1. From table 1, it is found that calculated values by AM1 & PM6 method are higher than the DFT values and DFT values are slightly higher than the HF method. The title molecule has total 54 bond lengths in which thirty C – C bond lengths, twenty-four C – H bond lengths. The highest bond length was calculated for $C_{26}H_{22}$ found to 1.520 Å. The calculated bond length values by B3LYP/6-31G (d, p) basis set for C-C bond in the title molecule vary from 1.391-1.520 Å and for C-H bond the values are in the range 1.084–1.096 Å [8]. Since the repulsive forces of the like charges (electron–electron, nucleus–nucleus) and the attractive forces of unlike charges (electrons–nucleus), we observe that the homo nuclear bond lengths are higher and hetero nuclear bond lengths are lower.

Table 1: bond lengths of Optimized structure of title molecule using AM1, PM6, HF/6-31g (d, p) and B3YLP/6-31g (d, p)

Bond	AM1	PM6	HF/6-31g	B3ylp/6-31g	Bond	AM1	PM6	HF/6-31g	B3ylp/6-31g
C_1-C_2	1.43	1.43	1.399	1.417	C_{14}-C_{16}	1.392	1.397	1.382	1.391
C_1-C_3	1.39	1.4	1.395	1.41	C_{14}-H_{29}	1.1	1.088	1.074	1.085
C_1-C_7	1.5	1.51	1.467	1.455	C_{15}-C_{17}	1.393	1.397	1.387	1.395
C_2-C_4	1.4	1.4	1.385	1.393	C_{15}-H_{30}	1.1	1.089	1.074	1.085
C_2-C_9	1.46	1.47	1.511	1.512	C_{16}-C_{18}	1.395	1.399	1.389	1.399
C_3-C_5	1.4	1.4	1.385	1.393	C_{16}-H_{31}	1.1	1.089	1.076	1.086
C_3-C_{39}	1.48	1.49	1.511	1.51	C_{17}-C_{18}	1.394	1.399	1.384	1.396
C_4-C_6	1.39	1.4	1.395	1.41	C_{17}-H_{32}	1.1	1.089	1.076	1.086
C_4-C_{43}	1.48	1.49	1.511	1.51	C_{18}-H_{33}	1.099	1.088	1.076	1.086
C_5-C_6	1.43	1.43	1.399	1.417	C_{19}-C_{20}	1.405	1.406	1.399	1.412
C_5-C_{10}	1.46	1.47	1.511	1.512	C_{19}-C_{21}	1.405	1.406	1.394	1.409
C_6-C_{12}	1.5	1.51	1.467	1.455	C_{20}-C_{22}	1.392	1.397	1.382	1.391
C_7-C_8	1.48	1.52	1.337	1.362	C_{20}-H_{34}	1.1	1.088	1.074	1.085
C_7-H_{25}	1.09	1.08	1.073	1.084	C_{21}-C_{23}	1.393	1.397	1.387	1.395
C_8-C_9	1.37	1.36	1.517	1.52	C_{21}-H_{35}	1.1	1.089	1.074	1.085
C_8-C_{13}	1.44	1.46	1.478	1.466	C_{22}-C_{24}	1.395	1.399	1.389	1.399
C_9-H_{26}	1.12	1.11	1.087	1.098	C_{22}-H_{36}	1.1	1.089	1.076	1.086
C_9-H_{48}	1.12	1.11	1.087	1.098	C_{23}-C_{24}	1.394	1.399	1.384	1.396
C_{10}-C_{13}	1.37	1.36	1.517	1.52	C_{23}-H_{37}	1.1	1.089	1.076	1.086
C_{10}-H_{27}	1.12	1.11	1.087	1.098	C_{24}-H_{38}	1.099	1.088	1.076	1.086
C_{10}-H_{47}	1.12	1.11	1.087	1.098	C_{39}-H_{40}	1.12	1.1	1.086	1.096

C_{11}-C_{12}	1.52	1.52	1.337	1.362	C_{39}-H_{41}	1.118	1.1	1.086	1.096
C_{11}-C_{19}	1.44	1.46	1.478	1.466	C_{39}-H_{42}	1.118	1.097	1.082	1.092
C_{12}-H_{28}	1.09	1.08	1.073	1.084	C_{43}-H_{44}	1.12	1.1	1.086	1.096
C_{13}-C_{14}	1.41	1.41	1.399	1.412	C_{43}-H_{45}	1.118	1.1	1.086	1.096
C_{13}-C_{15}	1.41	1.41	1.394	1.409	C_{43}-H_{46}	1.118	1.097	1.082	1.092

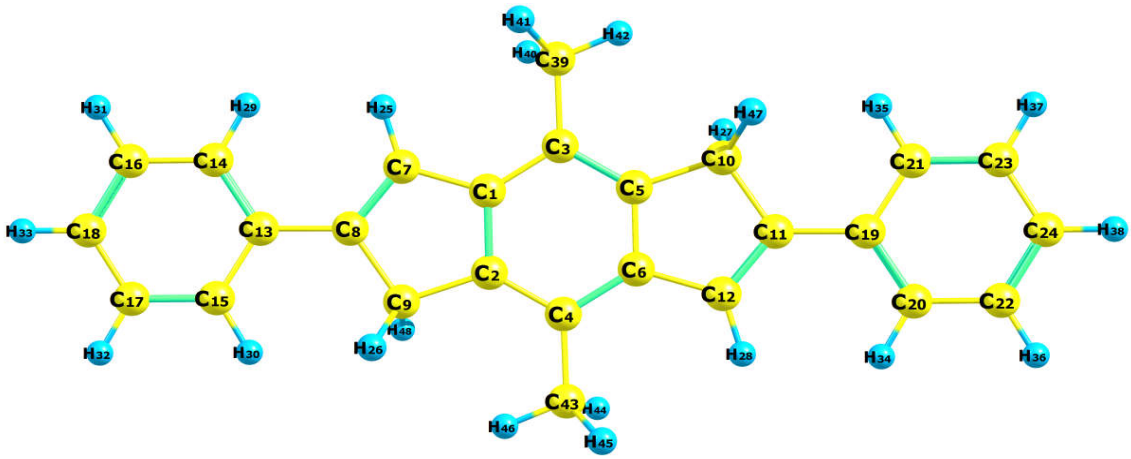

Figure 2: **Optimized structure of $C_{26}H_{22}$ (2, 6 di phenyl 4, 8 di methyl 1, 5 di hydro S-Indacene)**

3.2. Vibrational analysis

The vibrational spectral analysis of title molecule $C_{26}H_{22}$ using optimized structure in both neutral and in -1 oxidation state was performed to predict the vibrational frequencies, IR intensities and Raman activities. From the results it was observed that the frequencies calculated in theoretical methods were slightly greater than the characteristic frequencies in aromatic rings. For the better and accurate results and for the agreement between the theoretically calculated frequencies and characteristic frequencies, the computed harmonic frequencies are scaled for comparison using scaling factor.

Figure 3 and 4 shows the calculated IR and Raman spectra of the molecule ($C_{26}H_{22}$) in neutral and in -1 oxidation state. This molecule has 138 normal modes of fundamental vibrations calculated on the basis of 3N-6 formula, apart from three rotational and three translational degrees of freedom[9-11].

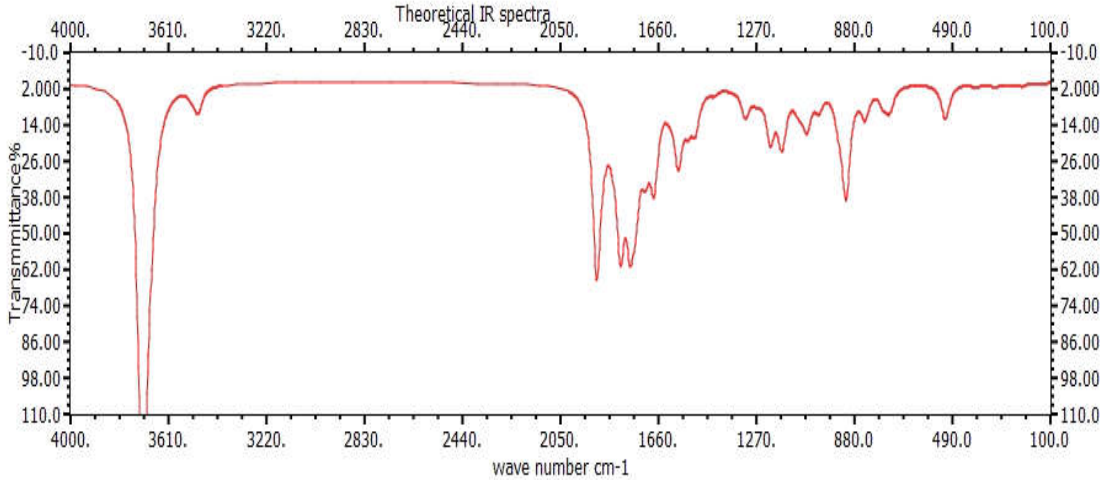

Figure 3(A): Theoretical IR spectra of $C_{26}H_{22}$ predicted by B3LYP/6-31G (d, p).

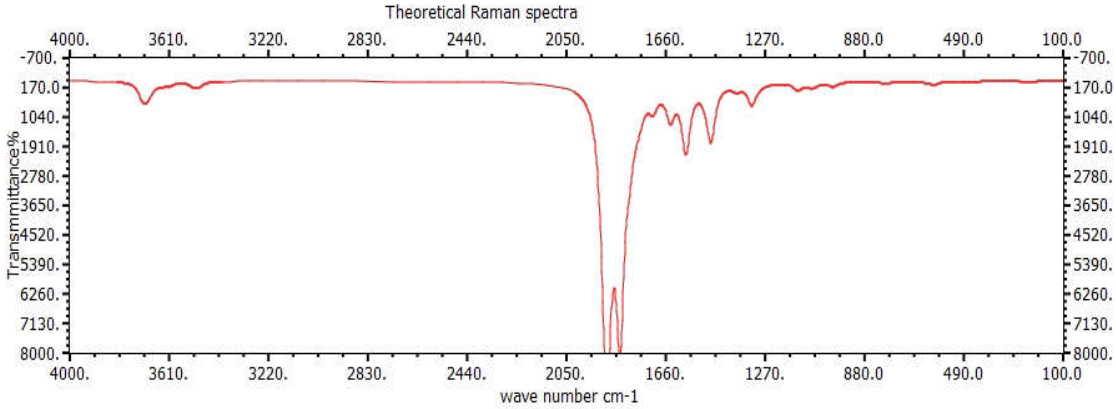

Figure 3(B): Raman spectra of $C_{26}H_{22}$ predicted by B3LYP/6-31G (d, p).

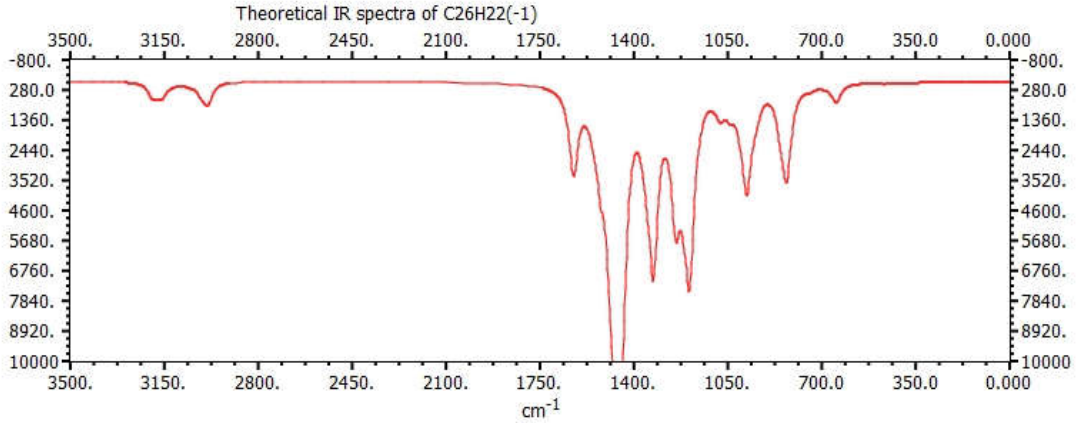

Figure 4(A): Theoretical IR spectra of $C_{26}H_{22}$ (-1) predicted by B3LYP/6-31G (d, p).

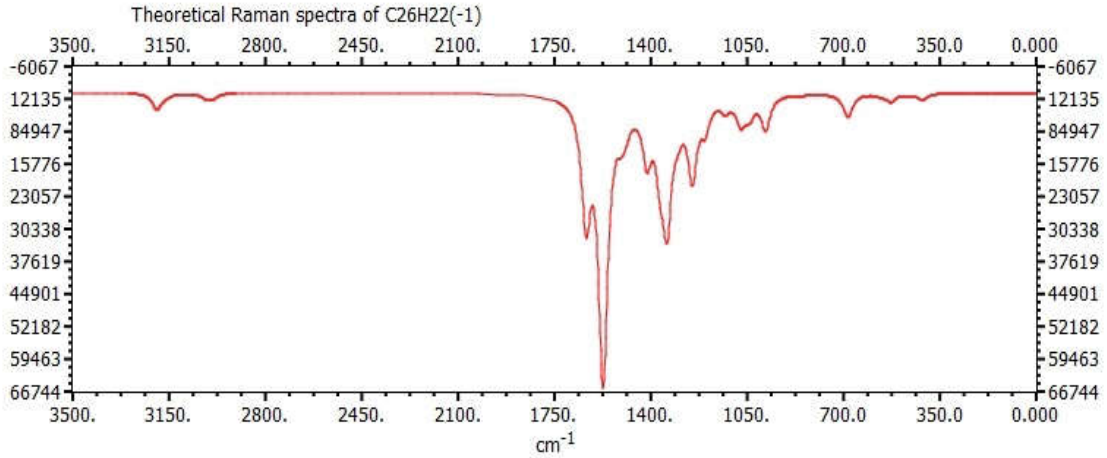

Figure 4(B): Raman spectra of $C_{26}H_{22}$ (-1) predicted by B3LYP/6-31G (d, p).

3.3 UV Spectral analysis

The chemical structure of $C_{26}H_{22}$ is consists of a conjugated system of single and double bonds of aromatic rings which gives the strong σ-σ * and π-π* transitions in the UV-Vis region with high extinction coefficients. The electronic spectra of $C_{26}H_{22}$ were computed for neutral and -1 oxidation state in the gas phase to predict the existence of absorption band in the near IR region due to electron delocalization. Using optimized ground state structure, TD-DFT/B3LYP/6-31G (d, p) calculations have been carried to determine the low-lying excited states of title molecule. The properties such as

the vertical excitation energies (E_{exc}), oscillator strength (f) and wavelength (λmax) were calculated. The λ_{max} is a function of substitution, stronger the electron releasing groups the larger λ_{max}.

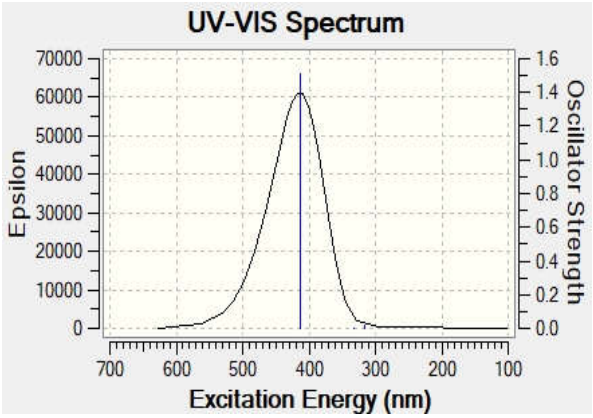

Figure 5 (A): UV spectra of $C_{26}H_{22}$

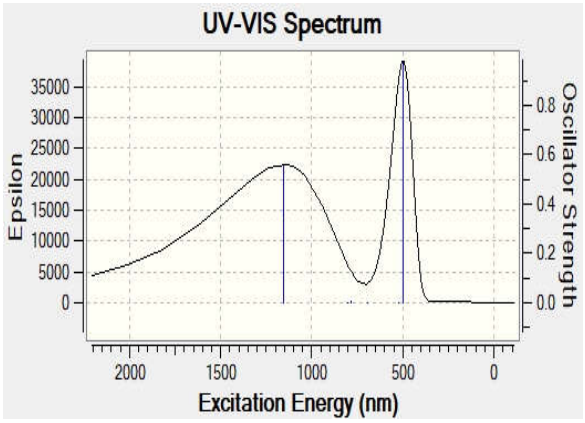

Figure 5(B): UV spectra of $C_{26}H_{22}$ (-1) predicted by B3LYP/6-31G (d, p).

UV spectra for the molecule in neutral and -1oxidation state predicted and are given in figure 4(A) and 4(B). UV spectrum of neutral $C_{26}H_{22}$ shows three transitions and absorption maxima (λ_{max}) observed at 413 nm with 1.5139 oscillator strength due to transition from HOMO (89) to LUMO (90) as shown in figure 4(A). Where as in case of $C_{26}H_{22}$ (-1) shows two transitions at wave lengths 1156 nm, 498 nm with oscillator strength 0.554 and 0.97 respectively. The existence of a band for anion $C_{26}H_{22}$ (-1) at 1156 nm in Near IR region indicates the presence of electron delocalization which is absent in case of neutral molecule $C_{26}H_{22}$. All electronic transitions, contribution of orbitals in transition and values of wavelengths, Energy and oscillator strengths values all are given in table 2.

Table 2: Energy, Wave lengths and orbital contribution in electronic transition of $C_{26}H_{22}$ [HOMO-90] and $C_{26}H_{22}$ (-1) [α HOMO- 90, β HOMO -89]

$C_{26}H_{22}$				C26H22(-1)			
Energy (cm-1)	**Wave-length (nm)**	**Osc. Strength**	**Major contribs/**	**Energy (cm-1)**	**Wave-length (nm)**	**Osc. Strength**	**Major contribs/**
24175	413	1.5139	HOMO->LUMO (100%) H-1->LUMO (11%),	8647	1156	0.554	HOMO(A)->LUMO(A) (97%)
				12459	802	0	HOMO(A)->L+1(A) (97%)
30158	331	0	HOMO->L+1 (88%)	12788	781	0.007	HOMO(A)->L+2(A) (99%)
31676	315	0.0205	H-2->LUMO (79%), HOMO->L+4 (15%),	14437	692	0	HOMO(A)->L+3(A) (95%)
				19161	521	0	HOMO(A)->L+4(A) (92%)
				20047	498	0.97	HOMO(B)->LUMO(B) (88%)

3.4 Study of effect of substituents in electronic properties:

In UV spectral analysis absorption maxima and oscillator strengths of title molecule have been reported in the table 3. In order to study the effect of the substituents in title molecule the electronic properties such as HOMO-LUMO energy gap, wave lengths (λ_{max}), oscillator strengths and energy values were calculated and given in table for the isolated molecule (S-Indacene) and Substituted derivatives of S-Indacene (structures are given figure 2). The UV-Vis spectra of all the structures were given in the figure 6. For all molecules charge -neutral and spin – singlet

Table 3: calculated HOMO-LUMO energy gap, wave lengths (λ_{max}), oscillator strengths and energy values

Struc-ture	**MF**	**No of atoms**	**No of molecules**	**Energy**	**HOMO**	**LUMO**	**Energy gap**	**Exit energy**		**Oscill strength**	
					eV	eV	eV	I^{st}	II^{nd}	I^{st}	II^{nd}
I(A)	C12H8	20	80	-462.08	-5.136	-3.018	2.118	474.14		0.1951	
I(B)	C14H12	26	96	-540.69	-5.024	-2.831	2.193	477.30		0.2687	
I(C)	C24H16	40	160	-924.173	-5.257	-2.823	2.434	490.52	454.02	0.1281	0.0598
I(D)	C26H20	46	176	-1002.83	-4.949	-3.033	1.916	485.87	449.31	0.1273	0.0583
I(E)	C26H22	48	178	-1004.08	-4.929	-1.606	3.323	413.66	315.69	1.5139	0.0205

In case of isolated S-Indacene molecule I(A) absorption maxima (λ_{max}) observed at 474.14 nm with oscillator strength 0.1951 and for 4,8 di methyl indacene I(B)λ_{max} at 477.3 nm and it is due presence of electron releasing groups (methyl) causes slightly increase in its wavelength. 2, 6 di phenyl indacene I(C) shows primary absorption bands at 490.52 and secondary absorption band at 454.02 nm. Since phenyl rings extended the conjugation and further increase the electron delocalization causes shift in absorption maxima to longer wavelength side (bathochromic shift). 4,8 dimethyl 2,6 diphenyl indacene I(D) give the two absorption bands at lower wave lengths 485.87 and 449.31 nm than the 2,6 di phenyl indacene I(C). The extended conjugation of π orbitals requires co-planarity of the atoms involved in the delocalization for maximum resonance interaction and causes increase in λ_{max}. But

due to the presence of methyl group in 4, 8 dimethyl 2, 6 diphenyl indacene I (D) causes a perturbation of the coplanarity of the ıı system, thus λ_{max} is usually shifted towards shorter wavelengths and oscillator strengths also decreases. Finally, in case of title molecule 4, 8 -dimethyl, 2, 6- diphenyl 1,-5 di hydro indacene absorption maxima (λ_{max}) observed at 413.66 with maximum oscillator strengths 1.5139. Presence of Hydrogens atoms at 1, 5 position loss its conjugation in ring system and increase the energy gap between HOMO-LUMO (3.323 eV) which causes decrease in wavelength. From the energy gap values given in table it can be explained that the larger the energy gap higher in the chemical stability of title molecule and lower in the chemical reactivity compared to the series of substituted derivatives of S-Indacene.

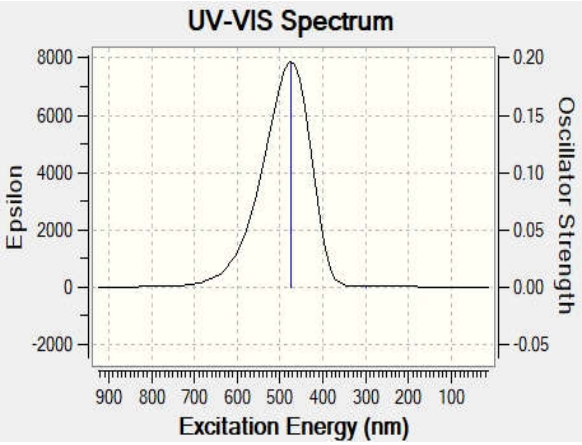

Figure 6(A): S-Indacene

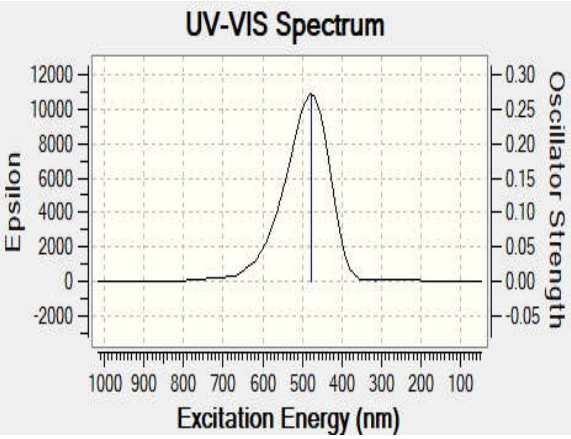

Figure 6(B): 4,8 di methyl indacene

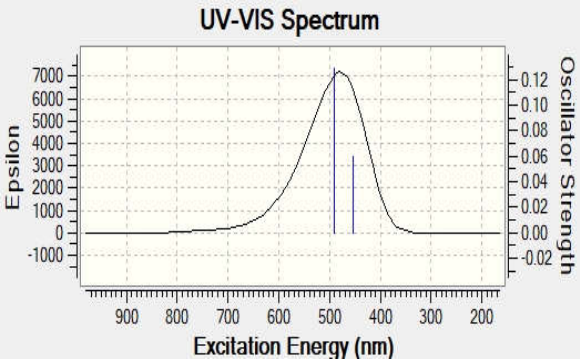

Figure 6(C): 2,6 di phenyl Indacene

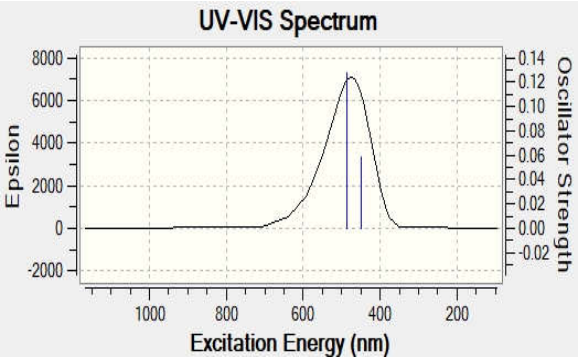

Figure 6(D): 4,8 di methyl 2,6 di phenyl Indacene

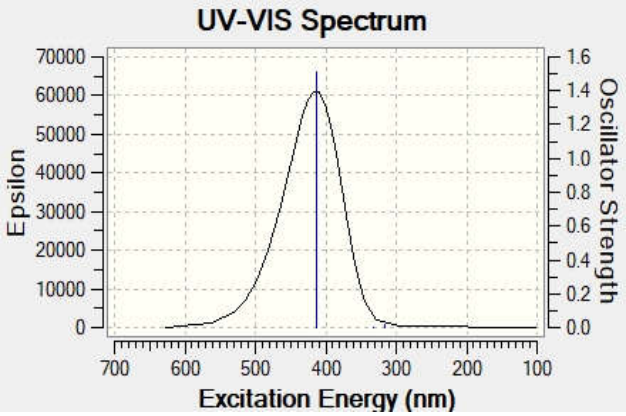

Figure 6(E): 4,8 di methyl 2,6 di phenyl 1,5 di hydro Indacene

Figure 6: The UV spectra of S indacene and its substituted derivatives

3.5. NMR spectral analysis:

NMR spectroscopy is used to find the nature of carbon and hydrogen atoms in order to elucidate the structure and molecular conformations. In theoretical chemistry GIAO/DFT (Gauge Including Atomic Orbitals/Density Functional Theory) approach is used to predict NMR spectra and to find the chemical shifts for various types of compounds [12-18].

Table 5: Chemical shift values (in ppm) of ^{13}C NMR, ^{1}H NMR Reference: TMS

Atom	B3LYP/6-31G(d,p)	Atom	B3LYP/6-31G(d, p)
C1	139.01	H25	7.72
C2	138.70	H26	3.67
C3	120.90	H27	3.67
C4	120.90	H28	7.72
C5	138.70	H29	8.09
C6	139.01	H30	7.58
C7	122.95	H31	7.55
C8	142.04	H32	7.52
C9	38.08	H33	7.34
C10	38.08	H34	8.09
C11	142.04	H35	7.58

C12	122.95	H36	7.55
C13	131.39	H37	7.52
C14	119.93	H38	7.34
C15	120.95	H40	2.48
C16	123.81	H41	2.48
C17	124.11	H42	2.27
C18	121.88	H44	2.48
C19	131.39	H45	2.48
C20	119.93	H46	2.27
C21	120.95	H47	3.67
C22	123.81	H48	3.67
C23	124.11		
C24	121.88		
C39	16.17		
C43	16.17		

Reference: TMS B3LYP/6-31G (d, p) GIAO,
Reference shielding: 192.06 ppm for ^{13}C , 31.75 ppm for ^{1}H.

NMR spectral analysis of $C_{26}H_{22}$ is carried out to predict ^{1}H and ^{13}C chemical shifts. Relative chemical shifts in terms of ppm were then estimated from ^{1}H and ^{13}C isotropic chemical shielding values using the TMS B3LYP/6-31G (d, p) reference shielding. The ^{1}H and ^{13}C theoretical chemical shifts values (in ppm) given in Table 5 and their resulting^{13}C and ^{1}H NMR spectra are presented as shown in Figure 7 & 8 .^{13}C NMR spectra exhibit signals in the downfield of 200 ppm depending on the structure. The external magnetic field experienced by the carbon nuclei is affected by the nature of the groups or atoms attached to them. The chemical shift values of aromatic carbon atoms of title molecules observed in the downfield at 142.04 and 142.04 ppm were attributed to C_8 and C_{11}, respectively. The other aromatic carbons C_3, C_4 observed in the up field at 120.90 ppm is due to +I effect of methyl group. The methylene carbon atoms C_9 and C_{10} of title molecule shows the peaks at 38.08 ppm. Aliphatic (methyl) carbons C39 and C43 shows chemical shift at 16.17ppm. The ring hydrogen atoms in $C_{26}H_{22}$ are assigned to the downfield chemical shift in range from 7.34- 8.09 ppm. Aliphatic hydrogens show chemical shift values in the up field region from 2.27-3.67 ppm

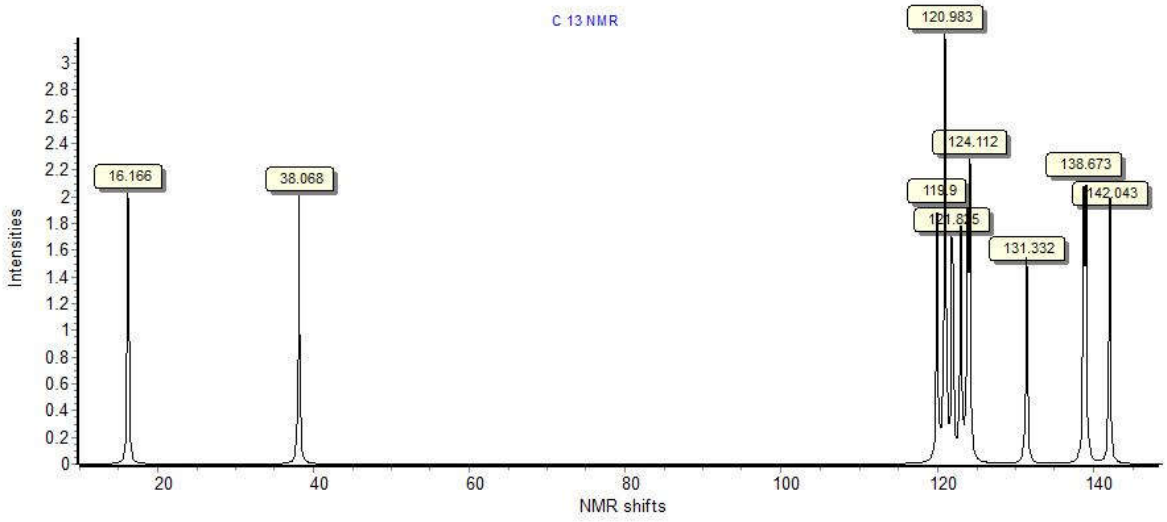

Figure 7: Theoretical C^{13} NMR spectra of $C_{26}H_{22}$ predicted by B3LYP/6-31G (d, p).

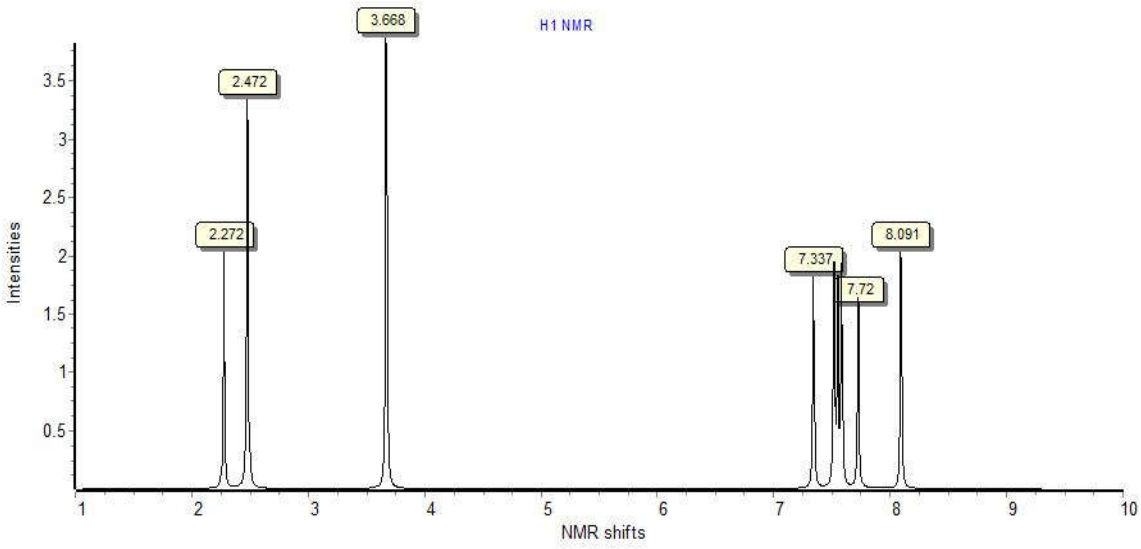

Figure 8: Theoretical H^1 NMR spectra of $C_{26}H_{22}$ predicted by B3LYP/6-31G (d, p).

3.6. Hyperpolarizability calculations:

Hyperpolarizability calculations of title molecule $C_{22}H_{26}$ involves the determination of first order hyperpolarizability (β_{total}) and its related properties dipole moment (μ) anisotropic polarizability (α) are determined by DFT/B3YLP method with 6–31G (d, P) basis set.

The total dipole moment of an isolated molecule in an electric field Ei(ω) can be represented as the $\mu_{total,}$ induced by the field.

$\mu_{tot} = \mu_0 + \alpha_{ij}E_j + \beta_{ijk}E_jE_k + \ldots..,$

Where α is the linear (isotropic) polarizability, $\mu_0$is the permanent dipole moment and β_{ijk} are the first hyperpolarizability tensor components. The isotropic linear polarizability is defined as: ¸
$\alpha = (\alpha_{xx} + \alpha_{yy} + \alpha_{zz})/ 3$

The first order hyperpolarizability (β) entire equation from Gaussian 09W output is given a follows:
$\beta_{tot=}$

$$\sqrt{(\beta xxx + \beta xyy + \beta xzz)2 + (\beta yyy + \beta yzz + \beta xxy)2 + (\beta zzz + \beta xxz + \beta yyz)2}$$

The calculations of first-order hyperpolarizability (β) and related properties such as dipole moment (μ) anisotropic polarizability α) using Gaussian 09 programe have been explained in detail previously[19-23]. In addition, the polar properties such as dipole moment and hyperpolarizability values from B3LYP/6-31G (d, p) method are given in Table 6.

Table 6: **The electric dipole moments (Debye), polarizability (in esu), β components and β tot (in esu) values calculated by B3LYP/6-31G (d, p) method**

Parameter	B3YLP	Parameter	B3YLP
μ_x	0	β_{XXX}	0
μ_y	0	β_{XXY}	0
μ_z	0.0883	β_{XYY}	0
μ_D	0.0883	β_{YYY}	0.0001
α_{XX}	-138.9695	β_{ZXX}	1.677

α_{XY}	1.3693	βXYZ	0.0273
α_{YY}	-134.1145	β_{ZYY}	0.3516
α_{XZ}	0	β_{XZZ}	0
α_{YZ}	-0.0002	β_{YZZ}	0
α_{ZZ}	-157.9908	β_{ZZZ}	0.1403
$\alpha_{i.p}$ (e.s.u)	0. 2130× 10−22	β_{tot} (e.s.u)	0.1874 × 10−31

3.7. Frontier orbital analysis:

3.7.1: HOMO-LUMO Energy gap:

Frontier orbital analysis is used to know HOMO-LUMO interactions. The calculation of energy gap between HOMO- LUMO is important to know the stability and reactivity of molecular structure [24]. The electronic properties such as total energy, HOMO-LUMO energies, energy gap (ΔE), the ionization potential (I), the electron affinity (A), the absolute electronegativity (χ), the absolute hardness (η) and softness (S) of the molecule $C_{22}H_{26}$ were calculated and given in Table 7.

The values of electronegativity, chemical potential, Chemical hardness, chemical softness and (Electrophilicity index) of title molecule can be calculated as follows:

$\chi = I+A/2$ (Electronegativity)
$\mu = -(I + A)/2$ (Chemical potential)
$\eta = I - A/2$ (Chemical hardness)
$s = 1/2\,\eta$ (chemical softness),
$\omega = \mu^2/2\,\eta$ (Electrophilicity index)

Where I and A are ionization potential and electron affinity; $I = -E_{HOMO}$ and $A = -E_{LUMO}$ respectively [25]. The lowest unoccupied molecular orbital (LUMO) energy is -1.6058 eV and the highest occupied molecular orbital (HOMO) energy is - 4.9286 eV. In DFT method, the energy gap of $C_{22}H_{26}$ is found to be as low as 3.3228 eV. This smaller energy gap of HOMO–LUMO is evident the electron transfer in the molecule, which influences its chemical reactivity, high polarizability and biological activities. In case of $C_{22}H_{26}$(-1) the energy gap between Alpha SOMO (90) and Alpha LUMO (91) is 1.4024 and in Beta orbitals SOMO (89) - LUMO (90) the energy gap is 3.3073, But the lowest energy gap is found between Alpha SOMO (90) - Beta LUMO (90) is 1.0953 eV. The smaller energy gap in $C_{22}H_{26}$ (-1) than in the neutral molecule $C_{22}H_{26}$. So excitations becomes easier as the HOMO-LUMO gap converges. Small HOMO-LUMO gaps in title molecule leads to mobile pi electrons since it is easy for the electron to jump to higher energy level that is close in energy. The greater the mobility of the π electrons, the greater the distribution of the energy throughout the molecule and stabilizing it. Hence smaller energy gap corresponds to the stability of the $C_{22}H_{26}$ (-1) molecule. Finally, in $C_{22}H_{26}$ (-2) the energy gap between Beta SOMO (90) and Beta LUMO (91) is 1.2811 eV which is greater than the energy gap in $C_{22}H_{26}$ (-1).

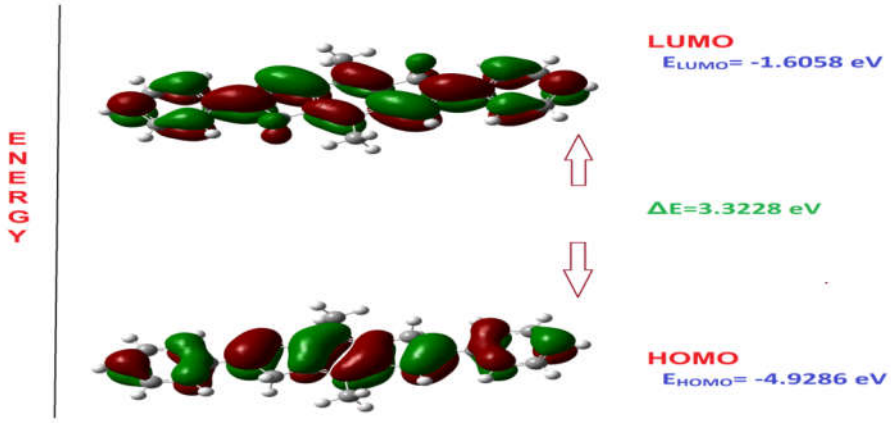

Figure 9: HOMO and LUMO of compound $C_{22}H_{26}$ calculated at B3LYP/6/31G (d, p) level

Table 7: Calculated values of title compound by B3LYP/6-31G (d, p) method

Basis set	**B3LYP/6-31G(d, p)**
E_{HOMO} (eV)	-4.929
E_{LUMO} (eV)	-1.606
Ionization potential	0.181
Electron affinity	0.059
Energy gap (eV)	0.122
Electronegativity	0.120
Chemical potential	-0.120
Chemical hardness	0.061
Chemical softness	0.031
Electrophilicity index	4.403

3.7.2. Total, sum of alpha plus beta electrons DOS:

Frontier orbital analysis not only involves HOMO-LUMO orbital but also involves the determination of total density of states (TDOS), and sum of α and β electron density of states[26,27]. The TDOS and α, β DOS of the compound $C_{22}H_{26}$ are given in Figs. 10 and 11. The importance of the DOS plots is to find Molecular orbital compositions and also provide the positive and negative charges with help of α β DOS, TDOS diagrams. The $C_{22}H_{26}$ molecule consists of totally 178 electrons, in which 89 α-electrons and 89 β-electrons were occupied in the density of states. A positive value of αβDOS displays a bonding interaction, negative value means anti-bonding interaction and zero value displays non-bonding interactions [28,29].

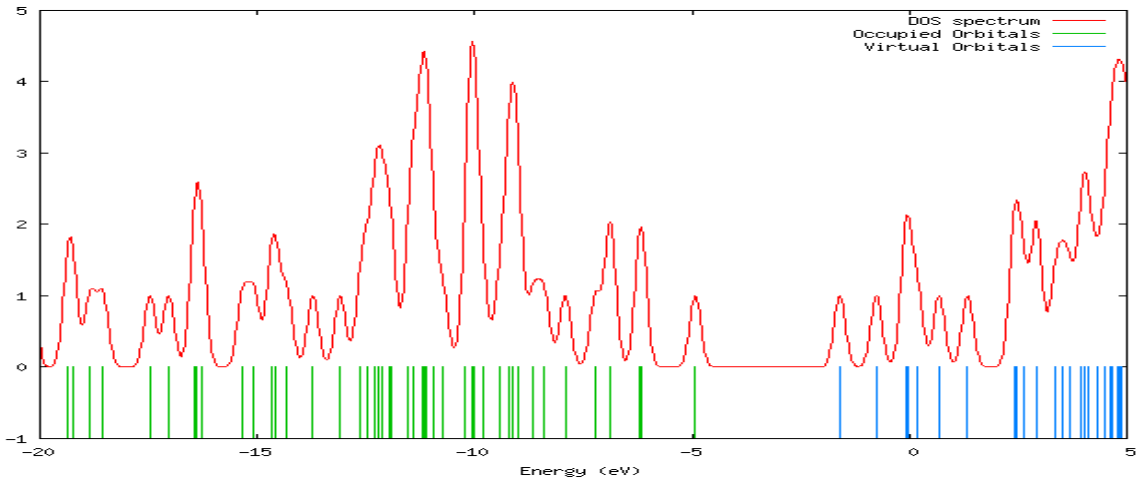

Figure 10: the calculated TDOS diagrams of $C_{22}H_{26}$

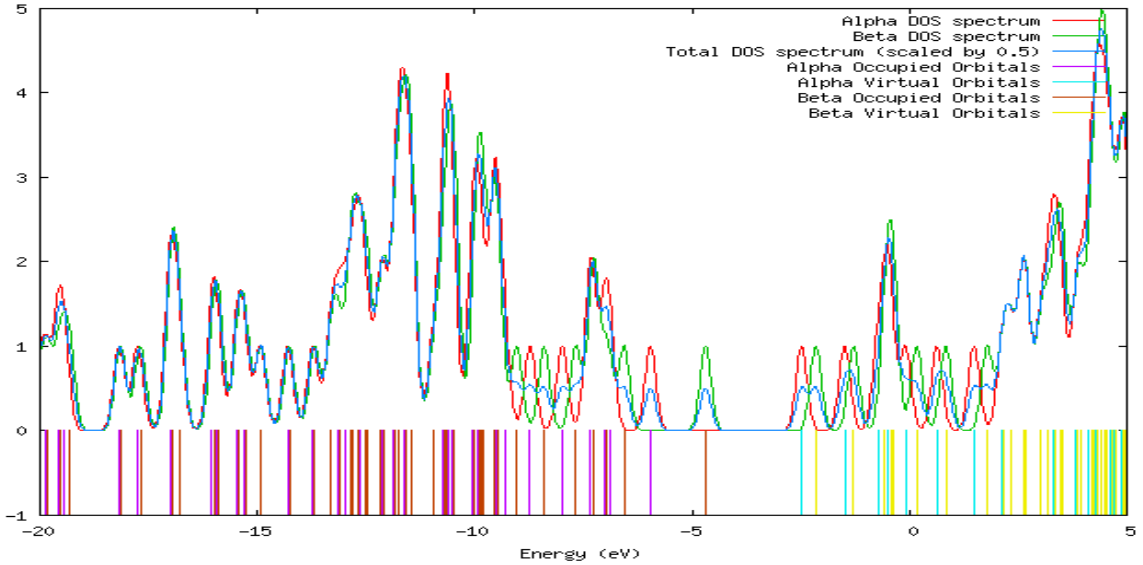

Figure 11: The calculated α β DOS diagram of $C_{22}H_{26}$ (-1)

3.8. Donor-Acceptor interactions from NBO Analysis:

In NBO analysis the second order fock matrix was carried out to know the interactions between donor-acceptor[30]. NBO analysis has been performed on the title molecule at the B3LYP/6-31G (d, p) level in order to elucidate the delocalization of electron density within the molecule. In case of larger E (2) value, the molecular interaction among electron donors and electron acceptors is very intensive. The strong intermolecular hyper conjugative interaction of π* (C19–C21) distributes to π *(C11–C12) of the ring and anti-bonding orbital π* (C13-C15) in the ring conjugate to the anti-bonding orbital of π *(C7–C8) which leads to strong delocalization of 97.53 and 97.53kJ/mol respectively. The high value of interaction energy, with large stabilization energy of 296.13 kJ/mol related to the resonance in the molecule is from anti-bonding donor π *(C5–C6) to the anti-bonding acceptor π * (C2–C4),as shown in table 8.

Table 8: Summarized results of NBO analysis for $C_{22}H_{26}$

No&. type Of NBO	Donor NBO (i)	ED/e	No. &. type Of NBO	Acceptor NBO (j)	ED/e	E2	E (j)-E (i) a.u.	F (i, j) a.u.
483. Π*	C19 - C21	0.03902	464. Π*	C11 - C12	0.0556	97.53	0.02	0.068
469. Π*	C13 - C15	0.03902	454. Π*	C7 - C8	0.0556	97.53	0.02	0.068
450. Π*	C5 - C6	0.05012	443. Π*	C2 - C4	0.0608	296.13	0.01	0.082
55. Π	C23 - C24	-0.243	483. Π*	C19 - C21	0.039	19.76	0.28	0.067
55. Π	C23 - C24	-0.243	485. Π*	C20 - C22	0.0399	19.93	0.28	0.068
48. Π	C20 - C22	-0.2452	483. Π*	C19 - C21	0.039	19.06	0.28	0.067
48. Π	C20- C22	-0.2452	492. Π*	C23 - C24	0.0382	19.24	0.28	0.066
46. Π	C19 - C21	-0.2389	464. Π*	C11 - C12	0.0556	15.39	0.29	0.063
46. Π	C19 - C21	-0.2389	485. Π*	C20 - C22	0.0399	18.71	0.28	0.066
46. Π	C19 - C21	-0.2389	492. Π*	C 23 - C24	0.0382	20.97	0.28	0.069
41. Π	C17 – C18	-0.243	469. Π*	C13 - C15	0.039	19.76	0.28	0.067
41. Π	C17 - C18	-0.243	471. Π*	C14 - C16	0.0399	19.93	0.28	0.068
34. Π	C14 - C16	-0.2452	469. Π*	C13 -C15	0.039	19.06	0.28	0.067
34. Π	C14 - C16	-0.2452	478. Π*	C17 - C18	0.0382	19.24	0.28	0.066
32. Π	C13 - C15	-0.2389	454. Π*	C7 - C8	0.0556	15.39	0.29	0.063
32. Π	C13 - C15	-0.2389	471. Π*	C14 - C16	0.0399	18.71	0.28	0.066
32. Π	C13 - C15	-0.2389	478. Π*	C17 - C18	0.0382	20.97	0.28	0.069
13 Π	C5 - C6	-0.2259	440. Π*	C1 - C3	0.0545	20.66	0.28	0.068
13.Π	C5 - C6	-0.2259	443. Π*	C2 - C4	0.0608	18.42	0.29	0.066
6. Π	C2 - C4	-0.2339	440. Π*	C1 - C3	0.0545	18.12	0.29	0.066
6. Π	C2 - C4	-0.2339	450. Π*	C5 - C6	0.0501	19.6	0.28	0.068
3. Π	C1 - C3	-0.2283	443. Π*	C2 - C4	0.0608	18.75	0.29	0.067
3. Π	C1 - C3	-0.2283	450. Π*	C5 - C6	0.0501	22.69	0.28	0.071

Where,
E (2) is the energy of hyper conjugative interaction (stabilization energy).
E (j)-E(i) is the energy difference between donor and acceptor i and j NBO orbitals.
F (i, j) is the Fock matrix element between i and j NBO orbitals.

3.9. Thermodynamical properties:
The thermodynamic properties such as heat capacity, entropy and enthalpy changes were computed from vibrational analysis at B3LYP/6-31G (d, p) basis set (at 1.0 atmospheres and 298.15K). The thermo chemistry output from Gaussian is summarized in Table 9. As observed from Table 8, the thermodynamic functions Cv, Cp, S, H, U and G values increasing with increase in temperature, ranges from 100 to 1000 K. This can be explained that the intensities of molecular vibrations increase with increase in temperature. The correlations between these thermodynamic properties (heat capacities, entropies, enthalpy changes) and temperatures (T) are shown in Fig. 12.

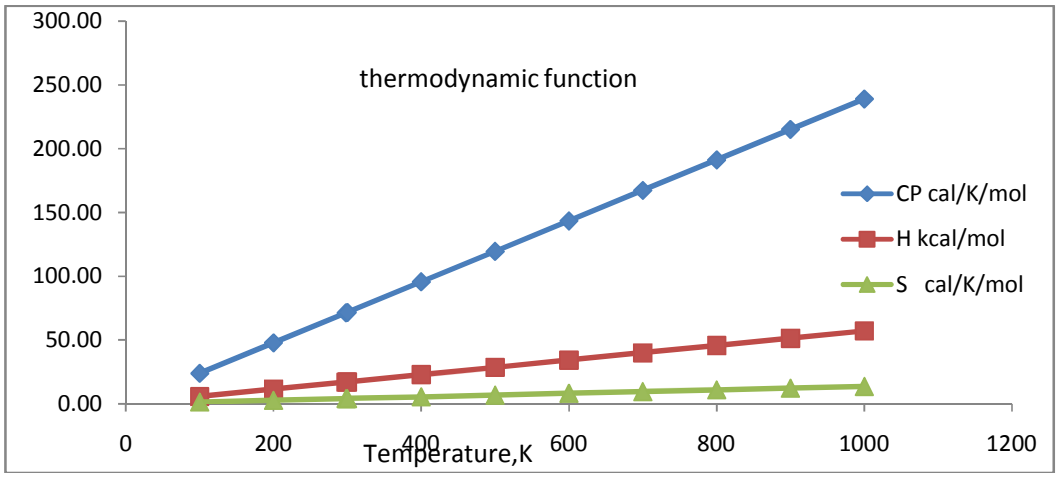

Figure 12: Variation of Thermodynamic properties of the title compound at B3LYP/6-31G (d, p).

The thermodynamic properties can be used to calculate the other thermodynamic energies and evaluate directions of chemical behavior according to the law of thermodynamics in the thermo chemical field [31].

Notice: All thermodynamic computations were done in the gas phase.

Table 9: Thermodynamic properties of $C_{22}H_{26}$ usingB3LYP/6-31G (d, P)

Temperature	Cv	Cp	U	H	S	G
K	cal/K/mol	cal/K/mol	kcal/mol	kcal/mol	cal/K/mol	kcal/mol
100	29.91	31.89	251.05	251.2	90.99	242.15
200	54.62	56.61	255.24	255.6	120.44	231.55
298.15	82.90	84.88	261.97	262.6	148.23	218.36
300	83.44	85.43	262.12	262.7	148.76	218.09
400	111.97	113.96	271.91	272.7	177.30	201.79
500	136.60	138.59	284.38	285.4	205.47	182.64
600	156.73	158.72	299.08	300.3	232.58	160.73
700	173.06	175.05	315.60	317.0	258.31	136.17
800	186.47	188.46	333.60	335.2	282.59	109.11
900	197.61	199.60	352.82	354.6	305.45	79.70
1000	206.98	208.97	373.06	375.0	326.98	48.07

3.10. Fukui function

Fukui function analysis has been carried out in UCA-FUKUI software using Gaussian output file, to calculate Fukui function, local softness and to identify the reactivity of the specific site in a molecule. only local parameters were calculated. Functions of Condensed Fukui (electrophilic, nucleophilic and radicular attack), Local Hardness and Electrophilicities (electrophilic and nucleophilic attack) are listed in table 10.

The Fukui function is defined as

$$f(\vec{r}) = (\partial\rho/\partial N)\upsilon(\vec{r}) = \left(\frac{\delta\mu}{\delta\upsilon(\vec{r})}\right)N$$

Kolandaival et al. [32], introduced the term atomic descriptor to determine the local reactive sites of the molecular system. Fukui function (f^{+}_{r}), (f^{-}_{r}) & (f^{0}_{r}) of atomic sites in title molecule have been listed in Table 10. Weitao Yangand Wilfried J. Mortier [33-35] have given a method to calculate the atomic Fukui function indices. Fukui functions were calculated using the following equation,

$f^{+}_{r} = q_r (N + 1) - q_r(N)$ for nucleophilic attack
$f^{-}_{r} = q_r(N) - q_r (N - 1)$ for electrophilic attack
$f_{r}^{0} = 1/2 (f^{+}_{r} + f^{-}_{r})$ for neutral (or radical) attack

In these equations, q_r is the atomic charge at the r^{th} atomic site is the anionic (N+1), cationic (N−1) chemical species.

Table 10: **Local Parameters table (Condensed Fukui f_r, dual descriptors, Local Hardness and Electrophilicities for $C_{22}H_{26}$**

N	f_r^-	f_r^+	f_r^0	Dual-Descriptor	Hardness (au)	W-(eV)	W+(eV)
1	0.1036	0.0595	0.0815	-0.044	0.0158	0.1762	0.1013
2	0.0392	0.0248	0.032	-0.0143	0.0058	0.0666	0.0422
3	0.0376	0.0328	0.0352	-0.0048	0.0051	0.064	0.0558
4	0.0376	0.0328	0.0352	-0.0048	0.0051	0.064	0.0558
5	0.0392	0.0248	0.032	-0.0143	0.0058	0.0666	0.0422
6	0.1036	0.0595	0.0815	-0.044	0.0158	0.1762	0.1013
7	0.06	0.0647	0.0623	0.0047	0.0073	0.102	0.1101
8	0.1261	0.1083	0.1172	-0.0178	0.017	0.2146	0.1842
9	0.0002	0.001	0.0006	0.0008	0	0.0004	0.0017
10	0.0002	0.001	0.0006	0.0008	0	0.0004	0.0017
11	0.1261	0.1083	0.1172	-0.0178	0.017	0.2146	0.1842
12	0.06	0.0647	0.0623	0.0047	0.0073	0.102	0.1101
13	0.0134	0.0333	0.0233	0.02	0.0004	0.0227	0.0567
14	0.0316	0.0389	0.0353	0.0073	0.0035	0.0538	0.0662
15	0.0325	0.0391	0.0358	0.0066	0.0037	0.0552	0.0665
16	0.0009	0.0041	0.0025	0.0032	-0.0001	0.0016	0.007
17	0.0026	0.0046	0.0036	0.0021	0.0002	0.0043	0.0079
18	0.0441	0.0609	0.0525	0.0168	0.0045	0.075	0.1036
19	0.0134	0.0333	0.0233	0.02	0.0004	0.0227	0.0567
20	0.0316	0.0389	0.0353	0.0073	0.0035	0.0538	0.0662
21	0.0325	0.0391	0.0358	0.0066	0.0037	0.0552	0.0665
22	0.0009	0.0041	0.0025	0.0032	-0.0001	0.0016	0.007
23	0.0026	0.0046	0.0036	0.0021	0.0002	0.0043	0.0079
24	0.0441	0.0609	0.0525	0.0168	0.0045	0.075	0.1036
26	0.0015	0.0115	0.0065	0.0099	-0.0004	0.0026	0.0195
27	0.0015	0.0115	0.0065	0.0099	-0.0004	0.0026	0.0195
39	0.0015	0.0008	0.0011	-0.0007	0.0002	0.0025	0.0014
40	0.0023	0.0049	0.0036	0.0026	0.0001	0.0039	0.0084
41	0.0023	0.0049	0.0036	0.0026	0.0001	0.0039	0.0084
43	0.0015	0.0008	0.0011	-0.0007	0.0002	0.0025	0.0014
44	0.0023	0.0049	0.0036	0.0026	0.0001	0.0039	0.0084

45	0.0023	0.0049	0.0036	0.0026	0.0001	0.0039	0.0084
47	0.0007	0.0056	0.0032	0.0049	-0.0002	0.0012	0.0095
48	0.0008	0.0062	0.0035	0.0053	-0.0002	0.0014	0.0105

Fukui functions in title molecule have been calculated for selected atomic sites and values are listed in Table 10. From table it has been found that C_8 and C_{11} has higher f^-_r, f^+_r values,which indicates the possible site for electrophilic and nucleophilic attack.

4. Conclusion

The equilibrium geometry of 4, 8 di methyl, 2, 6 di phenyl 1, 5 di hydro S-Indacene has been obtained at B3LYP /6-31G (d, p) basis set. IR and Raman spectra of title molecule were predicted with PED calculations regarding normal modes of vibrations. The first order hyperpolarizability calculation indicates the nonlinear optical properties of title molecule. C^{13} NMR and H^1 NMR chemical shift values are calculated using reference shielding value of TMS at 6-31G (d, p) basis set. The NBO analysis indicates the intramolecular charge transfer between the bonding and antibonding orbitals. Thermodynamic properties such as Enthalpy, entropy, heat capacity, internal energy and Gibb's free energy values in the range 100k to 1000k are obtained. The gradients of Cp, S and H increases, as temperature increases. Fukui functions helps to identifying the electrophilic/nucleophilic nature of specific site within a molecule. The molecule orbital contributions were studied by using the total density of states. UV spectral analysis of the title molecule predicts the existences absorption band in near IR region makes this molecule is an interesting object for further studies. Furthermore, study shows the large energy gap due to the effect of the substituents and hence we conclude that this molecule has better thermodynamic and kinetic stability.

5. References

1. K. Hafner, Maja Nendela, Bernd Goldfussa, K.N. Houka, s-Indacene, a quasi-delocalized molecule with mixed aromatic and anti-aromatic character Theochem. 1999, 461 -462, 23-28
2. R. Shahidha , S. Muthu , M. Raja , R. Raj Muhamed , B. Narayana , Prakash S. Nayak , B.K. Sarojini Spectroscopic (FT-IR, FT-Raman), first order hyperpolarizabilities, NBO, Fukui function and molecular docking study of N-(4-Chloro-3-methylphenyl)-2-phenylacetamide. Optik: International Journal for Light and Electron Optics, 2017,140, 1127(16)
3. S. Muthu, G. Ramachandran, Spectroscopic studies (FTIR, FT-Raman and UV-Visible), normal coordinate analysis, NBO analysis, first order hyper polarizability, HOMO and LUMO analysis of (1R)-N-(Prop-2-yn-1-yl)-2,3-dihydro-1H-inden-1-amine molecule by ab initio HF and density functional methods. Spectrochim. Acta A ,2014,121, 394–403
4. R. Srinivasaraghavan, S. Thamaraikannan, S. Seshadri, T. Gnanasambandan, Molecular conformational stability and Spectroscopic analysis of Parared with experimental techniques and quantum chemical calculations. Spectrochim. Acta A , 2015,137 ,1194–1205.
5. H.B. Stiegel, Optimization of equilibrium geometries and transition structures. J. Comput. Chem. 1982, 3(2), 214–218.
6. C. Lee, W. Yang, R.G. Parr, Development of the Colle-Salvetti correlation-energy formula into a functional of the electron density. Phys. Rev.1988, B 37, 785–789.
7. M. Frisch, G. Trucks, H. Schlegel, G. Scuseria, M. Robb, J. Cheeseman, T. Vreven, K. Kudin, J. Burant, J. Millam, S.S. Iyengar, J. Tomasi, V. Barone, B.Mennucci, M. Cossi, G. Scalmani, N. Rega, H. G.A. Petersson, M. Nakatsuji, M. Hada, K. Ehara, R. Toyota, M.I.J. Fukuda, T. Hasegawa, Y. Nakajima, O. Honda, H. Kitao, M. Nakai, X. Klene, J. Li, H.P. Knox, J. Hratchian, V. Cross, C. Bakken, J. Adamo, R. Jaramillo, R. Gomperts, O. Stratmann, A. Yazyev, R. Austin, C. Cammi, J. Pomelli, P. Ochterski, K. Ayala, G. Morokuma, P. Voth, J. Salvador, V. Dannenberg, A.D.S. Zakrzewski, M. Dapprich, O. Strain, D.Farkas, A. Malick, K. Rabuck, J. Raghavachari, J. Foresman, Q. Ortiz, A. Cui, S. Baboul, J. Cliord, G.L.B.B. Cioslowski, A. Stefanov, P. Liashenko, I. Piskorz, R. Komaromi, D. Martin, T. Fox, M. Keith, C.P. Al-Laham, A. Nanayakkara, M. Challacombe, P. Gill, W.C.B. Johnson, M. Wong, C. Gonzalez, J. Pople, Gaussian 03, Revision E.01, Gaussian Inc, Wallingford, 2004.

8. A. Frisch, A. Nielsen, A. Holder, Gaussview User's Manual, Gaussian Inc., Pittsburgh, 2007.
9. N.M. O'Boyle, A.L. Tenderholt, K.M. Langner. A Library for Package-Independent Computational Chemistry Algorithms. J. Comp. Chem. 2008, 29, 839–845.
10. P.L. Polavarapu, Ab initio vibrational Raman and Raman optical activity spectra J. Phys. Chem. 1990, 94, 8106–8112.
11. E.B. Wilson, J.C. Decius, P.C. Cross, Molecular Vibrations: The Theory of Infrared and Raman Vibrational Spectra, Dover Publ. Inc, Newyork, 1980.
12. A. Jayaprakash, V. Arjunan, S.P. Jose, S. Mohan, Vibrational and electronic investigations, thermodynamic parameters, HOMO and LUMO analysis on crotonaldehyde by ab initio and DFT methods. Spectrochim. Acta, 2011, 83A, 411–419.
13. P. Pulay, G. Fogarasi, F. Pang, J.E. Boggs, Systematic ab initio gradient calculation of molecular geometries, force constants, and dipole moment derivatives, J. Am. Chem. Soc. 1979,101, 2550–2560.
14. Ozgur Alver, Cemal Parlak, and Mustafa Şenyel, NMR spectroscopic study and DFT calculations of giao nmr shielding and 1JC-H spin-spin coupling constants of 1, 9-diaminononane. Chem. Soc. Ethiop. 2009, 23(1), 85-96.
15. Krushelnitsky, A.; Reichert, D. Complex 1H,13C-NMR relaxation and computer simulation study of side-chain dynamics in solid polylysine. Biopolymers, 2005, 78(3), 129.
16. Krushelnitsky, A.; Reichert, D. Prog. NMR spectroscopy in liquids and solids, NMR Spectrosc. 2005, 47, 1.
17. Senyel, M.; Alver, O.; Parlak, C. NMR Spectroscopic Study And Dft Calculations Of Vibrational Analyses, Giao Nmr Shieldings And $^{1}J_{C\text{-}H}$, $^{1}J_{C\text{-}C}$ Spin-Spin Coupling Constants Of 1,7-Diaminoheptane Spectrochim. Acta A 2008, 71, 830.
18. Parlak C, Alver O, Senyel M, FT-IR and NMR investigation of 1-phenylpiperazine: a combined experimental and theoretical study. Spectrochim. Acta A 2006, 67(3-4), 793-801.
19. Zhang Y, Li, T, Teng.Q, Theoretical Study on Electronic Structures and Spectroscopy of Triarylborane Substituted By Thiophene. Bull. Chem. Soc. Ethiop. 2009, 23, 77.
20. Barone. G, Paloma. L.G, Duca, D, Silvestri. A, Riccio. R, Bifulco. G, Structure validation of natural products by quantum-mechanical GIAO calculations of 13C NMR chemical shifts. Chem. Eur. J. 2002, 8, 3233.
21. D. Sajan, I.H. Joe, V.S. Jajakumar, J. Zaleski, Structural and electronic contributions to hyperpolarizability in methyl p-hydroxy benzoate J. Mol. Struct. 2006, 785(1-3), 43–53.
22. K.S. Thanthiri Watte, K.M. Nalin de silva, Non-linear optical properties of novel fluorenyl derivatives—ab initio quantum chemical calculations. J.Mol. Struct. Theochem. 2002, 617, 169–175.
23. S.G. Sagdinc, A. Esme, NMR, UV-Visible, NLO, NBO, MEP and Vibrational Spectroscopic (IR and Raman) Analysis, Spectrochim. Acta A, 2010, 75, 1370–1380.
24. D.F.V. Lewis, C. Loannides, D.V. Parke, Interaction of a series of nitriles with the alcohol-inducible isoform of P450: Computer analysis of structure—activity relationships Xenobiotica, 1994, 24, 401–408.
25. R.G. Pearson, Absolute electronegativity and hardness correlated with molecular orbital theory.Proc. Natl. Acad. Sci. 1986, 83, 8440–8441.
26. R. Hoffmann, Solids and Surfaces: A Chemist's View of Bonding in Extended Structures, VCH Publishers, New York, 1988.
27. J.G. Małecki, Synthesis, crystal, molecular and electronic structures of thiocyanate ruthenium complexes with pyridine and its derivatives as ligands, Polyhedron, 2010, 29, 1973–1979.
28. E. Rutherford, Philos. Mag. 47 (284) (1899) 9.
29. M. Chen, U.V. Waghmare, C.M. Friend, E. Kaxiras, A density functional study of clean and hydrogen-covered α-MoO_3(010): Electronic structure and surface relaxation. J. Chem. Phys. 1998,109, 6854–6860.
30. Pulay P, Fogarasi G, Ponger G, Boggs JE, Vargha A. Combination of theoretical ab initio and experimental information to obtain reliable harmonic force constants. Scaled quantum mechanical (QM) force fields for glyoxal, acrolein, butadiene, formaldehyde, and ethylene. J. Am. Chem. Soc.1983, 105, 7037-7047.

31. Fogarasi G, Zhou X, Taylor PW, Pulay P. The calculation of ab initio molecular geometries: efficient optimization by natural internal coordinates and empirical correction by offset forces. J. Am. Chem. Soc.1992, 114, 8191-8201.
32. Kolandaivel P, Praveen G, Selvarengan P. Study of atomic and condensed atomic indices for reactive sites of molecules. J. Chem. Sci.2005, 11, 591-598.
33. S. Muthu, E. Isac Paulraj, Spectroscopic and molecular structure (monomeric and dimeric structure) investigation of 2-[(2-hydroxyphenyl) carbonyloxy] benzoic acid by DFT method: A combined experimental and theoretical study. J. Mol. Struct. 2013, 1038, 145–162.
34. Weitao Yang, Wilfried J. Mortier, The use of global and local molecular parameters for the analysis of the gas-phase basicity of amines.J. Am. Chem. Soc. 1986, 108, 5708–5711.
35. Sun YX, Hao QL, Wei WX, Yu ZX, Lu LD, Wang X, Wang YS. Experimental and density functional studies on 4-(3, 4- dihydroxybenzylideneamino) antipyrine, and 4-(2, 3, 4-trihydroxybenzylideneamino) antipyrine. J. Mol. Struct. (Theochem.) 904, 2009, 74-82.